ACS APPLIED MATERIALS & INTERFACES

Letter

www.acsami.org

Ionic Transport through Chemically Functionalized Hydrogen Peroxide-Sensitive Asymmetric Nanopores

Mubarak Ali,[*,†,‡] Ishtiaq Ahmed,[§] Saima Nasir,[†,‡] Patricio Ramirez,[∥] Christof M. Niemeyer,[§] Salvador Mafe,[⊥] and Wolfgang Ensinger[†]

[†]Department of Material- and Geo-Sciences, Materials Analysis, Technische Universität Darmstadt, D-64287 Darmstadt, Germany

[‡]Materialforschung, GSI Helmholtzzentrum für Schwerionenforschung, D-64291 Darmstadt, Germany

[§]Institute for Biological Interfaces (IBG-1), Karlsruhe Institute of Technology (KIT), Hermann-von-Helmholtz-Platz, D-76344 Eggenstein-Leopoldshafen, Germany

[∥]Departament de Física Aplicada, Universitat Politécnica de València, E-46022 València, Spain

[⊥]Departament de Física de la Terra i Termodinàmica, Universitat de València, E-46100 Burjassot, Spain

Supporting Information

ABSTRACT: We describe the fabrication of a chemical-sensitive nanofluidic device based on asymmetric nanopores whose transport characteristics can be modulated upon exposure to hydrogen peroxide (H_2O_2). We show experimentally and theoretically that the current−voltage curves provide a suitable method to monitor the H_2O_2−mediated change in pore surface characteristics from the electronic readouts. We demonstrate also that the single pore characteristics can be scaled to the case of a multipore membrane whose electric outputs can be readily controlled. Because H_2O_2 is an agent significant for medical diagnostics, the results should be useful for sensing nanofluidic devices.

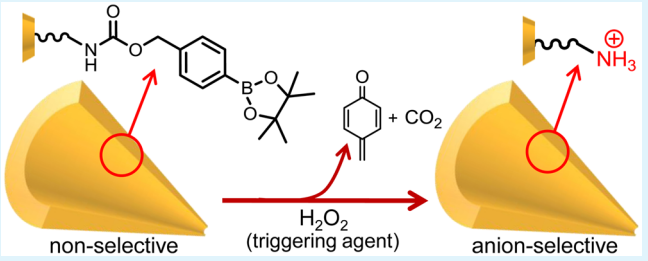

KEYWORDS: *asymmetric nanopores, chemical functionalization, H_2O_2-sensitive pore, current rectification, Nernst−Planck equations*

In this letter, we describe the chemical functionalization of hydrogen peroxide (H_2O_2)-sensitive asymmetric nanopores, showing experimentally and theoretically that the current−voltage (I−V) curves of a single pore provide a suitable method to monitor the solution properties from electronic readouts. We demonstrate also the scalability of the single pore characteristics to the case of a multipore membrane whose output electrical signals can be readily controlled. The surface functionalization process suggests the possibility of reusing the pores while the scalability paves the way to integration into functional devices through multipore membranes. Note that H_2O_2 is an agent significant for medical diagnostics,[1−5] which is usually monitored by biological, chemical, and electrochemical methods based on spectrometry,[4,6] chemoluminescence,[7,8] and amperometry.[9,10] An alternative method is based on confining the sensing process within a single nanopore whose inner surface is functionalized, e.g., with the covalently linked enzyme horseradish peroxidase.[11] The changes observed in the I−V curves can then be correlated with the presence of H_2O_2 in the external solution. High sensor sensitivities can be achieved because of the small working volume and the off-the-shelf electronic equipment.[12] Moreover, different techniques have been developed in order to tune the pore surface chemistry for efficient control over ionic transport across the membrane.[12−20] The design of a nanopore sensitive to a chemical (e.g., H_2O_2) under physiological conditions still constitutes a challenge for current techniques.

The asymmetric track-etching technique[21] was employed here to fabricate the asymmetric nanopores in polyethylene terephthalate (PET) membranes of thickness 12 μm. Both single pore and multipore (1×10^4 pores/cm^2) membranes were obtained by heavy ion irradiation and subsequent chemical track-etching process (see the Supporting Information for experimental details). The resulting carboxylic acid (−COOH) groups were exposed on the pore surface.[13] These groups act as starting points for the covalent attachment of different functionalities which modulate the electrochemical characteristics of the pore surface (Figure 1a−d).

To fabricate the hydrogen peroxide sensitive nanopore, we have synthesized an amine-terminated boronic ester carbamate (**6**) (BEC−NH_2) compound (see the Supporting Information for detail). Briefly, the starting material 4-(4,4,5,5-tetramethyl-1,3,2-dioxaborolan-2-yl)benzylalcohol (**1**) was first synthesized in excellent yield by already reported method.[22] Then, the activation of benzyl alcohol (**1**) was performed with carbonyldiimidazol (**2**) in anhydrous acetonitrile to give a stable imidazole carbamate (**3**).[23] Subsequently, the reaction of *N*-

Received: July 6, 2015
Accepted: August 27, 2015
Published: August 27, 2015

DOI: 10.1021/acsami.5b06015
ACS Appl. Mater. Interfaces 2015, 7, 19541−19545

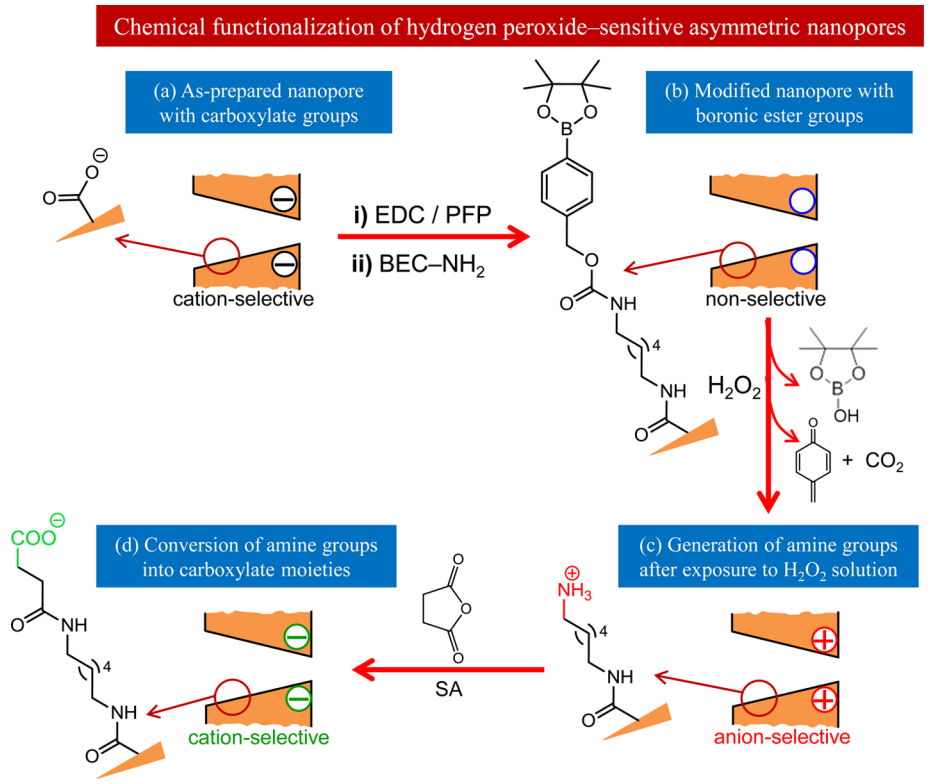

Figure 1. (a, b) Surface functionalization of the carboxylic acid groups with amine-terminated boronic ester carbamate (BEC-NH_2) moieties via carbodiimide coupling chemistry. (b, c) H_2O_2 triggered generation of amine groups on the pore surface. (c, d) Conversion of surface amine groups into carboxylic acids moieties by reaction with succinic anhydride (SA).

boc-1,6-hexanediamine (**4**) with imidazole carbamate (**3**) gave *N*- boc-protected carbamate (**5**). The protected carbamate (**5**) was treated with trifluoroacetic acid in dichloromethane (1:3) to give the BEC−NH_2 (**6**) compound.

The covalent functionalization of the BEC−NH_2 on the pore surface was achieved through *N*-(3-(dimethylamino)propyl)-*N*′-ethylcarbodiimide/pentafluorophenol (EDC/PFP) coupling chemistry (Figure 1a, b).[12] Finally, the surface amine groups were converted into carboxylic acids moieties by reaction with succinic anhydride (SA) as shown in Figure 1c, d (see Scheme S2 for more detail).[16]

Figure 2a shows the *I*−*V* curves of a single asymmetric nanopore before and after the functionalization of the H_2O_2 sensitive molecules on the inner pore surface (Figure 1a, b). The rectification characteristics, defined as the ratio $|I(+2\ V)|/|I(-2\ V)|$ in the inset by taking in account the negative pore surface polarity, arise from the electrostatic interaction of the asymmetrically distributed surface charge with the mobile ions in solution.[14] The *I*−*V* curves were obtained under symmetrical electrolyte conditions using a nonbuffered 0.1 M KCl solution at pH = 5.6 ± 0.2 in the conductivity cell. The as-prepared, unmodified asymmetric pore is cation selective (Figure 1a) and rectifies the ionic current (Figure 2a). The preferential direction of cation flow is from the narrow tip toward the wide opening.[14,24] After modification, the anchoring of the BEC−NH_2 neutral chains having uncharged terminal boronic ester decreased the pore surface charge density, in agreement with the significant decrease observed in the pore rectification ratio, from 5.7 to 1.7.

Figure 1b, c shows the generation of amine groups upon exposing the BEC-modified pore to a solution of H_2O_2. The slightly alkaline solution of H_2O_2 can hydrolyze the arylboronic ester into a corresponding phenol.[25] The resulting phenolic compound further undergoes decarboxylation and 1,6-elimination reactions, leading to the generation of amine groups (Scheme S3).[26] H_2O_2 acts as a triggering agent which generates the amine groups on the backbone of the boronic ester carbamate chains.[26] Figure 2b shows the *I*−*V* curves of the BEC-modified pore when exposed to a H_2O_2 solution of concentration 800 μM for different times. As expected, an inversion of the ionic current rectification[14,24] with respect to that of Figure 2a was observed due to the amine moieties on the pore surface (in our experimental conditions, the amine groups are protonated, imparting positive charge to the pore surface). This process also leads to the conversion of the inner pore environment from a hydrophobic nonconducting state to a hydrophilic conducting state.

Figure 2b suggests that the exposure time to the H_2O_2 solution was proportionally related to the generation of amine groups, which changes the pore rectification and ionic current. After 60 min of exposure time, the value of positive current was decreases while that of the negative current increased (in absolute value) compared with the reference values of the BEC-modified pore. Further increase in the exposure time enhanced the above experimental trends because of the increased pore surface charges. However, after 180 min of exposure time, no significant change in the positive and negative ion currents was observed, indicating the saturation of the surface charge.

As discussed above, the pore rectification is directly related with the H_2O_2-dependent surface charge density (Figure 1b, c). The rectification ratio in the inset of Figure 2b, estimated from the corresponding *I*−*V* curves as $|I(-2\ V)|/|I(+2\ V)|$ by keeping in mind the positive pore surface polarity, was then regulated by the pore exposition to H_2O_2. This fact provides a

DOI: 10.1021/acsami.5b06015
ACS Appl. Mater. Interfaces 2015, 7, 19541−19545

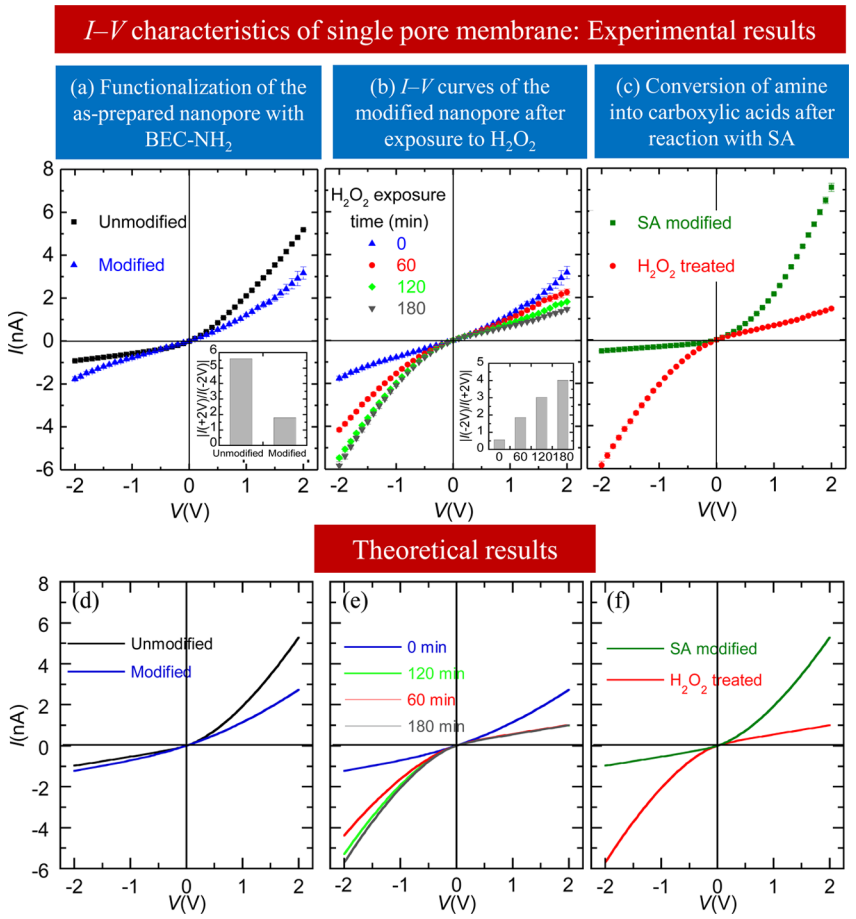

Figure 2. (a) $I-V$ curves of a single asymmetric nanopore with approximate tip and opening diameters $2a_R \approx 25 \pm 3$ nm and $2a_L \approx 600 \pm 10$ nm, respectively, in a 100 mM KCl solution at pH 5.6 ± 0.2. The inset shows the rectification ratios for the same pore prior to (black) and after (blue) chemical modification. (b) $I-V$ curves of the modified nanopore in electrolyte solution before (blue) and after exposure to H_2O_2 for 60 (red), 120 (green), and 180 (black) minutes. The inset shows the rectification ratios as a function of the H_2O_2 exposure time. (c) $I-V$ curves of the H_2O_2 treated nanopore in solution prior to (red) and after (green) reaction with SA (in most of the measurements the error bars are equal to or smaller than symbol size). (d–f) Theoretical $I-V$ curves obtained from eqs 1 and 2 corresponding to the experimental conditions in a–c.

facile tool to correlate the presence of H_2O_2 in solution to the system electronic readout. Indeed, upon exposing the modified pore to the H_2O_2 solution for 60, 120, and 180 min, the electrical rectification ratio increased to 1.9, 3.0 and 4.0, respectively, to be compared with the unmodified pore value (0.5).

Figure 1c, d shows that the arylboronic ester hydrolysis and subsequent generation of amine groups triggered by H_2O_2 can be further modified through a chemical reaction between the terminal amine groups and succinic anhydride (SA) molecules. When the H_2O_2 treated, aminated pore is exposed to SA, condensation reactions lead to the production of terminal carboxylate groups on the pore surface. After SA modification, the regenerated carboxylate moieties switch the surface charge from positive to negative, changing the pore ionic selectivity and rectification from anionic to cationic (Figure 2c). The carboxylic acid moieties on the SA-modified pore surface suggest the possibility of reusing the pore (Figure S1).

The above experimental results can be described theoretically using a continuous approach based on the Poisson and Nernst–Planck equations[15,27–30]

$$\nabla^2\phi = -\frac{F}{\varepsilon}\sum_i z_i c_i \tag{1}$$

$$\nabla\vec{J}_i = -\nabla\left[D_i\left(\nabla c_i + z_i c_i \frac{F}{RT}\nabla\phi\right)\right] = 0 \tag{2}$$

where $c_i(x)$, z_i, $\vec{J}_i$, and D_i, are the local concentration, charge number, flux density, and diffusion coefficient of ion i, respectively, with $\phi(x)$ being the local electric potential and ε the electrical permittivity. In eq 2, T is the absolute temperature, with F and R being the Faraday and universal gas constants, respectively. The pore radius at a point of coordinate x along the pore axis is described by the equation

$$a(x) = \frac{a_R - a_L\exp[-(d/h)^n] - (a_R - a_L)\exp[-(x/d)^n(d/h)^n]}{1 - \exp[-(d/h)^n]} \tag{3}$$

where d is the pore length and parameters n and d/h control the pore shape.[28] eqs 1–3 can be integrated numerically to give the ionic flux densities, and then the total electric current I through the nanopore, at each applied voltage V (see references22 and26 for details). The above model is useful to describe the $I-V$ curves of different nanopores[15,27–30] using a reduced number of fitting parameters. Figure 2d–f shows that this is also the case of the present experimental results. The best fitting between theory and experiments has been found using $d/h = 0$ and $n = 1.25$ in the calculations, which gives a pore profile with a convex tip,[28] slightly deviated from a perfect conical shape. Once the pore shape has been determined, the

DOI: 10.1021/acsami.5b06015
ACS Appl. Mater. Interfaces 2015, 7, 19541–19545

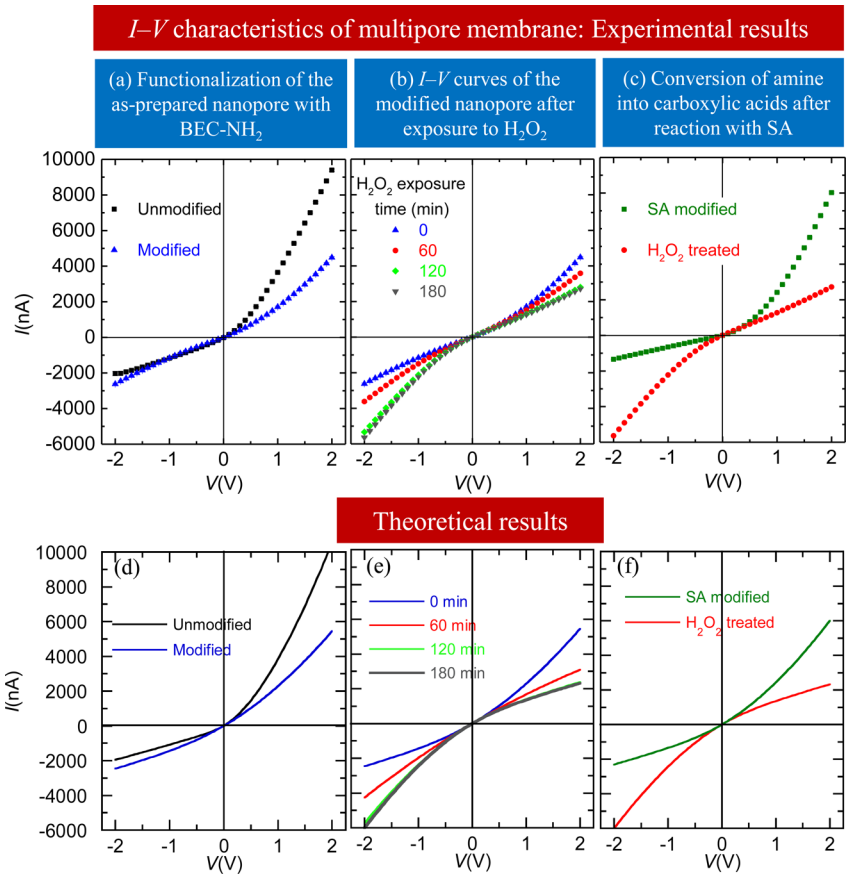

Figure 3. (a) $I-V$ curves of a multipore membrane with 1×10^4 asymmetric pores/cm^2 prior to (black) and after (blue) modification with BEC-NH_2 groups. (b) $I-V$ curves of a modified multipore membrane before (blue) and after exposition to a H_2O_2 solution for a period of 60 (red), 120 (green) and 180 (black) min. (c) $I-V$ curves of a H_2O_2 treated multipore membrane prior to (red) and after (green) reaction with SA. All measurements were carried out in a nonbuffered 100 mM KCl solution at pH 5.6 ± 0.2 (in most of the measurements the error bars are equal to or smaller than symbol size). (d–f) Theoretical $I-V$ curves obtained from eqs 1 and 2 corresponding to the experimental conditions in a–c.

only free parameter in the theoretical curves is the surface charge density σ(in units e/nm^2, where e is the elementary charge). The values of σ used in the calculations were −0.3, −0.06, (Figure 2d, unmodified and modified pore, respectively), − 0.06, + 0.2, + 0.28, and +0.35 (Figure 2e, 0, 60, 120, and 180 min of H_2O_2 exposure, respectively), and −0.3 and +0.35 (Figure 2f, SA modified and H_2O_2 treated pore, respectively). These values are reasonable, as shown previously with these types of pores.[27,28]

Finally, Figure 3a–c shows the $I-V$ curves of a multipore membrane containing ∼10^4 asymmetric pores/cm^2 approximately. This membrane was etched along with the same single-pore membrane used in the functionalizations discussed above. The experimental results suggested that the ionic transport across the multipore membrane can be controlled using similar conditions to those of the single-pore membrane (Figure 2a–c). Indeed, the $I-V$ curves of Figure 3a reveal that the number of open pores contributing to the electric current was approximately 2×10^3/cm^2. The surface functionalization method developed for the single-pore membrane can then be integrated and exploited in multipore nanofluidic devices. The scalability characteristics should be useful for practical applications. Figure 3d–f shows that the theoretical curves can reproduce the experimental trends observed assuming the same pore shape as in the single pore experiments, with σ (in e/nm^2) = −0.3 and −0.06 (Figure 3d, unmodified and modified pore, respectively), − 0.06, + 0.02, + 0.07 and +0.08 (Figure 3e, 0 min, 60 min, 120 and 180 min of H_2O_2 exposure, respectively), and −0.06 and +0.08 (Figure 3f, SA modified and H_2O_2 treated pore, respectively). Note that the experiments in Figure 3b show that the negative currents after the H_2O_2 exposure were slightly lower (in absolute value) than the positive currents characteristic of the as prepared pore (Figure 3a). This is not the case for the single pore sample in Figure 2, where these negative currents in Figure 2b were slightly higher than those characteristic of the as-prepared pore in Figure 2a. As a result, the values of σ found for the multipore membrane are significantly lower than those found for the single pore sample. It might be possible that upon refixing of the sample in the conductivity cell after succinic anhydride treatment, the membrane area exposed to electrolyte solution contains fewer pores, leading to a decrease in ion current flowing across the membrane.The nanopores in the track-etched membrane are randomly distributed because of nonuniform heavy ion irradiation of polymer foil.

In summary, we have described the chemical functionalization of H_2O_2-sensitive asymmetric nanopores, showing experimentally and theoretically that the $I-V$ curves provide a suitable method to monitor the solution properties from electronic readouts. Also, we have demonstrated the scalability of the single pore characteristics to a multipore membrane whose output could be readily controlled, a crucial step to miniaturize and develop useful nanofluidic devices.

DOI: 10.1021/acsami.5b06015
ACS Appl. Mater. Interfaces 2015, 7, 19541−19545

■ ASSOCIATED CONTENT

Supporting Information

The Supporting Information is available free of charge on the ACS Publications website at DOI: 10.1021/acsami.5b06015.

Experimental detail for the chemical synthesis of amine-terminated boronic ester carbamate (BEC-NH_2) compound, fabrication of track-etched nanopore and functionalization procedures (PDF)

■ AUTHOR INFORMATION

Corresponding Author

*E-mail: M.Ali@gsi.de.

Notes

The authors declare no competing financial interest.

■ ACKNOWLEDGMENTS

M.A., S.N. and W.E. acknowledge the funding from the Hessen State Ministry of Higher Education, Research and the Arts, Germany, under the LOEWE project iNAPO. P.R. and S.M. acknowledge the support from the Ministry of Economic Affairs and Competitiveness and FEDER (project MAT2012-32084) and the Generalitat Valenciana (project Prometeo/GV/0069 for Groups of Excellence). I.A. and C.M.N. acknowledge financial support through the Helmholtz programme Bio-Interfaces in Technology and Medicine. The authors are thankful to Prof. C. Trautmann, Department of Materials Research from GSI, for support with irradiation experiments.

■ REFERENCES

(1) Barnham, K. J.; Masters, C. L.; Bush, A. I. Neurodegenerative Diseases and Oxidative Stress. *Nat. Rev. Drug Discovery* **2004**, *3*, 205−214.

(2) Dickinson, B. C.; Chang, C. J. A Targetable Fluorescent Probe for Imaging Hydrogen Peroxide in the Mitochondria of Living Cells. *J. Am. Chem. Soc.* **2008**, *130*, 9638−9639.

(3) Finkel, T.; Serrano, M.; Blasco, M. A. The Common Biology of Cancer and Ageing. *Nature* **2007**, *448*, 767−774.

(4) Jin, H.; Heller, D. A.; Kalbacova, M.; Kim, J. H.; Zhang, J. Q.; Boghossian, A. A.; Maheshri, N.; Strano, M. S. Detection of Single-Molecule H2O2 Signalling from Epidermal Growth Factor Receptor using Fluorescent Single-Walled Carbon Nanotubes. *Nat. Nanotechnol.* **2010**, *5*, 302−309.

(5) Lin, M. T.; Beal, M. F. Mitochondrial Dysfunction and Oxidative Stress in Neurodegenerative Diseases. *Nature* **2006**, *443*, 787−795.

(6) Dickinson, B. C.; Huynh, C.; Chang, C. J. A Palette of Fluorescent Probes with Varying Emission Colors for Imaging Hydrogen Peroxide Signaling in Living Cells. *J. Am. Chem. Soc.* **2010**, *132*, 5906−5915.

(7) Chen, W. W.; Li, B. X.; Xu, C. L.; Wang, L. Chemiluminescence Flow Biosensor for Hydrogen Peroxide using DNAzyme Immobilized on Eggshell Membrane as a Thermally Stable Biocatalyst. *Biosens. Bioelectron.* **2009**, *24*, 2534−2540.

(8) Tahirovic, A.; Copra, A.; Omanovic-Miklicanin, E.; Kalcher, K. A Chemiluminescence Sensor for the Determination of Hydrogen Peroxide. *Talanta* **2007**, *72*, 1378−1385.

(9) Bustos Bustos, E.; Chapman, T. W.; Rodriguez-Valadez, F.; Godinez, L. A. Amperometric Detection of H2O2 using Gold Electrodes Modified with Starburst PAMAM Dendrimers and Prussian Blue. *Electroanalysis* **2006**, *18*, 2092−2098.

(10) Kausaite-Minkstimiene, A.; Mazeiko, V.; Ramanaviciene, A.; Ramanavicius, A. Enzymatically Synthesized Polyaniline Layer for Extension of Linear Detection Region of Amperometric Glucose Biosensor. *Biosens. Bioelectron.* **2010**, *26*, 790−797.

(11) Ali, M.; Tahir, M. N.; Siwy, Z.; Neumann, R.; Tremel, W.; Ensinger, W. Hydrogen Peroxide Sensing with Horseradish Peroxidase-Modified Polymer Single Conical Nanochannels. *Anal. Chem.* **2011**, *83*, 1673−1680.

(12) Ali, M.; Nasir, S.; Ramirez, P.; Ahmed, I.; Nguyen, Q. H.; Fruk, L.; Mafe, S.; Ensinger, W. Optical Gating of Photosensitive Synthetic Ion Channels. *Adv. Funct. Mater.* **2012**, *22*, 390−396.

(13) Ali, M.; Ramirez, P.; Mafe, S.; Neumann, R.; Ensinger, W. A pH-Tunable Nanofluidic Diode with a Broad Range of Rectifying Properties. *ACS Nano* **2009**, *3*, 603−608.

(14) Guo, W.; Tian, Y.; Jiang, L. Asymmetric Ion Transport through Ion-Channel-Mimetic Solid-State Nanopores. *Acc. Chem. Res.* **2013**, *46*, 2834−2846.

(15) Nasir, S.; Ramirez, P.; Ali, M.; Ahmed, I.; Fruk, L.; Mafe, S.; Ensinger, W. Nernst-Planck Model of Photo-Triggered, pH-Tunable Ionic Transport through Nanopores Functionalized with "Caged" Lysine Chains. *J. Chem. Phys.* **2013**, *138*, 034709.

(16) Vlassiouk, I.; Siwy, Z. S. Nanofluidic Diode. *Nano Lett.* **2007**, *7*, 552−556.

(17) Chen, W.; Wu, Z.-Q.; Xia, X.-H.; Xu, J.-J.; Chen, H.-Y. Anomalous Diffusion of Electrically Neutral Molecules in Charged Nanochannels. *Angew. Chem., Int. Ed.* **2010**, *49*, 7943−7947.

(18) Gao, H.-L.; Zhang, H.; Li, C.-Y.; Xia, X.-H. Confinement Effect of Protonation/Deprotonation of Carboxylic Group Modified in Nanochannel. *Electrochim. Acta* **2013**, *110*, 159−163.

(19) Li, S.-J.; Li, J.; Wang, K.; Wang, C.; Xu, J.-J.; Chen, H.-Y.; Xia, X.-H.; Huo, Q. A Nanochannel Array-Based Electrochemical Device for Quantitative Label-free DNA Analysis. *ACS Nano* **2010**, *4*, 6417−6424.

(20) Gao, H.-L.; Wang, M.; Wu, Z.-Q.; Wang, C.; Wang, K.; Xia, X.-H. Morpholino-Functionalized Nanochannel Array for Label-Free Single Nucleotide Polymorphisms Detection. *Anal. Chem.* **2015**, *87*, 3936−3941.

(21) Apel, P. Y.; Korchev, Y. E.; Siwy, Z.; Spohr, R.; Yoshida, M. Diode-Like Single-Ion Track Membrane Prepared by Electro-Stopping. *Nucl. Instrum. Methods Phys. Res., Sect. B* **2001**, *184*, 337−346.

(22) Filippis, A. d.; Morin, C.; Thimon, C. Synthesis of some Para-Functionalized Phenylboronic acid Derivatives. *Synth. Commun.* **2002**, *32*, 2669−2676.

(23) Broaders, K. E.; Grandhe, S.; Fréchet, J. M. J. A Biocompatible Oxidation-Triggered Carrier Polymer with Potential in Therapeutics. *J. Am. Chem. Soc.* **2011**, *133*, 756−758.

(24) Siwy, Z. S. Ion-Current Rectification in Nanopores and Nanotubes with Broken Symmetry. *Adv. Funct. Mater.* **2006**, *16*, 735−746.

(25) Kuivila, H. G.; Armour, A. G. Electrophilic Displacement Reactions. IX. Effects of Substituents on Rates of Reactions between Hydrogen Peroxide and Benzeneboronic Acid1−3. *J. Am. Chem. Soc.* **1957**, *79*, 5659−5662.

(26) Lo, L.-C.; Chu, C.-Y. Development of Highly Selective and Sensitive Probes for Hydrogen Peroxide. *Chem. Commun.* **2003**, 2728−2729.

(27) Cervera, J.; Schiedt, B.; Neumann, R.; Mafe, S.; Ramirez, P. Ionic Conduction, Rectification, and Selectivity in Single Conical Nanopores. *J. Chem. Phys.* **2006**, *124*, 104706.

(28) Ramirez, P.; Apel, P. Y.; Cervera, J.; Mafe, S. Pore Structure and Function of Synthetic Nanopores with Fixed Charges: Tip Shape and Rectification Properties. *Nanotechnology* **2008**, *19*, 315707.

(29) Ramirez, P.; Cervera, J.; Ali, M.; Ensinger, W.; Mafe, S. Logic Functions with Stimuli-Responsive Single Nanopores. *ChemElectroChem* **2014**, *1*, 698−705.

(30) Ramirez, P.; Gomez, V.; Ali, M.; Ensinger, W.; Mafe, S. Net Currents Obtained from Zero-Average Potentials in Single Amphoteric Nanopores. *Electrochem. Commun.* **2013**, *31*, 137−140.

DOI: 10.1021/acsami.5b06015
ACS Appl. Mater. Interfaces 2015, 7, 19541−19545